MINISTRY OF EDUCATION AND TRAINING
HANOI PEDAGOGICAL UNIVERSITY 2

LE HONG VIET

STUDY ON THERMODYNAMIC PROPERTY OF DEFECTIVE TERNARY AND BINART ALLOYS WITH FACE-CENTERED CUBIC AND BODY-CENTERED CUBIC STRUCTURES

Speciality: Mathematical and Theoretical Physics
Code: 9 44 01 03

SUMMARY OF PhD THESIS

HANOI - 2022

This work is completed at Hanoi Pedagogical University 2

Scientific supervisor 1: Assoc. Prof. PhD. Nguyen Quang Hoc

Scientific supervisor 2: PhD. Pham Thi Minh Hanh

Reviewer 1: Prof. Dr. Sci Nguyen Huu Tang

Reviewer 2: Prof. PhD. Do Dinh Thanh

Reviewer 3: Assoc. Prof. PhD. Nguyen Hong Quang

The thesis will be defended at the University-level thesis evaluation Council at Hanoi Pedagogical University 2 at the hour... date...month... year 2022

The thesis is available at

- Hanoi National Library
- Library of Hanoi Pedagogical University 2

INTRODUCTION

1. Reasons for choosing the topic

Interstitial alloys are one of the materials that have a strategic role in military, science and technology and materials technology such as superconducting materials, electricity and electronics, nuclear, space, metallurgy, jewelry and medical devices. These lightweight, durable, high-temperature and high-pressure alloys are widely used in the weapons, rockets, spacecraft, aircraft and automobile industries. Alloys with high chemical and mechanical strength are used in the manufacture of equipment in the petroleum and chemical industries. Stainless alloys are used to make medical tools and kitchen utensils. Beautiful and hard alloy of gold, silver and copper used to make jewelry.

Defects in general and vacancies in particular have a very important influence on the properties of metals and alloys at high temperatures. Equilibrium vacancy concentrations at melting point have orders of magnitude about 10^{-3} in low-melting metals and 10^{-2} in high-melting-point metals. The strong nonlinear effects in heat capacity and thermal expansion at high temperatures can be explained by the formation of point defects. At high pressures above 100 GPa, another type of defect is dislocation, which contributes significantly to the melting temperature of the crystal.

Computational thermodynamics is a core component of computational materials science because thermodynamic properties are the most fundamental and can have a major influence on kinetic properties and material handling process.

There are many theoretical methods to study the vacancy and thermodynamic properties of metals and alloys such as the planar wave method of *ab initio* combined with psido-harmonic Debye model, *ab*

initio calculation combined with generelized gradient approximation, *ab initio* combines density functional theory with generalized gradient approximation, approach of co-existence phases, calculation of phase diagram, lattice Green function method, modified embedded atomic method, machine learning method, etc. Each method has its own advantages and disadvantages when applied to multi-component systems at high temperature and pressure. Most of the methods to study the thermodynamic properties of metals and alloys are approximations, not taking into account the anharmonicity effect in lattice vibrations, usually only at zero and low pressure. low pressure, not taking into account the dependence of thermodynamic quantities on the concentrations of substituted and interspersed atoms. The results of theoretical methods to study thermodynamic properties are mostly for metals and limited for alloys. Some results obtained from theoretical methods are not really consistent with experiments. Statistical moment method (SMM) is a modern physical method of statistical physics that can be applied to study thermodynamic, elastic, diffusion, phase transition, melting,... for many types of materials with different structures in the temperature range from absolute zero to the melting point of the material and under pressure, including pressure as high as hundreds of GPa. SMM has been successfully applied to study defective metals and substitutional alloys. However, the study of the effect of defects on the thermodynamic, melting and structural phase transition properties of binary interstitial alloys, ternary substitutional and interstitial alloys with cubic structures by SMM is an open issue. This method hopes to overcome the disadvantages mentioned above of other methods.

With the above reasons, I choose the topic of the thesis as *"Study on thermodynamic properties of defective ternary and binary interstitial alloys with face-centered and body-centered cubic structures".*

2. Purpose, object and scope of research

Applying SMM to study the thermodynamic, melting and structural phase transition properties of cubic defective interstitial alloy AC and substitutional and interstitial alloy ABC taking into account the influence of temperature, pressure, concentration of substitutional atoms, concentration of interstitial atoms and concentration of equilibrium vacancies.

The object of study is the thermodynamic properties of cubic defective interstitial alloy AC and substitutional and interstitial alloy ABC.

The research scope in the ranges of temperature, pressure, concentration of substitutional atoms, concentration of interstitial atoms and concentration of equilibrium vacancies corresponds to the experiment.

3. Research methods

The main research method is the statistical moment method. In addition, in numerical calculations we use the Maple sofware and approximate methods such as approximate iteration.

4. Scientific and practical significance

The results from the thesis provide a lot of information about the thermodynamic, melting àn structural phase transition properties of interstitial alloy such as the dependence on temperature, pressure, concentration of components and concentration of equilibrium vacancies of the thermal expansion coefficient, the heat capacity at constan pressure, the melting temperature, the structural phase transition temperature, etc. The thesis contributes to the development of SMM in studying the properties of interstitial alloy materials

5. New contributions of thesis

Build analytic expressions for thermodynamic quantities, melting temperature and structural phase transition temperature of cubic defective interstitial alloy AC and substitutional and interstitial alloy ABC using SMM. The thesis contributes to supplementing and perfecting the theory of the equilibrium vacancy and cubic interstitial alloy.

Apply the obtained theory to calculate numerically for metals and alloys. The obtained numerical results are compared with the experimental data and the results calculated by other theoretical methods. Some numerical results can be predictive and guide future experiments.

6. Thesis outline

In addition to the Introduction, the Conclusion, the References and the Appendixes, the thesis content is presented in 4 chapters.

CHAPTER 1
OVERVIEW OF RESEARCH OBJECT AND METHODS

In chapter 1, we introduce interstitial alloy, vacancy theory and some theoretical methods in studying thermodynamic properties of metals and alloys. All methods have advantages and disadvantages when applied to metals and alloys. Especially, we present the SMM and explain why this method is chosen as the research method of the thesis.

1.1. Interstitial alloy

In interstitial alloy, metal is the main component, usually 90% or more. The other components are non-metallic. It is an alloying agent and usually accounts for less than 1% concentration. The most important nonmetals are C, H, O and N. The crystal structure of interstitial alloy is determined by the parent metal.

1.1.1. Binary interstitial alloy with cubic structure

Fe's interstitial alloys such as FeSi, FeC and FeH give us information about the composition, structure, evolution ... of the Earth and celestial bodies. FeC called carbon steel accounts for a large proportion in the steel industry. The substitutional alloy FeCr is widely used in nuclear reactors and wear-resistant stainless engineering materials. Interstitial alloys AuSi and CuSi have attracted the attention of researchers in recent years because of their wide application in superconducting wire fabrication, jewelry, bearing assembly, ballast, casting, step welding and radiation shielding. The study of TaSi and WSi alloys was determined by calculating the phase diagram. Knowing the phase diagram and thermodynamic properties of the TaSi, WSi systems has an important technical role for the metal contacts between Ta, W and SiC in electrical and electronic devices.

Alloys such as AuSi and CuSi attract the interest of researchers due to their applications and unusual physical properties.

The thermodynamic, elastic, melting and diffusing properties of the perfect alloys FeSi, FeC, FeH, WSi, AuSi, CuSi and AgC have been studied by SMM in recent years.

1.1.2. Substitutional and interstitial ternary alloy with cubic structure

Zhang *et al* [*Physica B: Condensed Matter*, 586(2020) 412085] studied the influence of Si on the Debye temperature and the thermal expansion coefficient of FeCr, in which the Young's modulus of FeCrSi increased with the increase of Cr concentration. Pogatscher *et al*. [*Physical Review Letters*, 112(22) (2014) 225701] studied equilibrium vacancies concentration to control aging mechanisms of AlMgSi alloys. It is the most widely used of aluminum alloys with industrial applications such as construction, automobiles, aircraft, rockets, spacecraft and architecture. Li *et al* [*Chemical Society Reviews*, 46(6)(2017)1693] studied the effect of vacancy on materials with different structures such as those for making electrodes of lithium batteries in clean energy storage, sodium ion and catalyst to separate hydrogen from water. Zhang et al [*Computational Materials Science*, 148(2018)249] studied point defects, equilibrium defect concentration to improve the performance of irradiated materials. Recently, the thermodynamic, elastic and melting properties of the perfect alloys FeCrSi, FeCrC, AuCuSi and AuCuLi have been investigated by SMM.

1.2. Vacancy theory and theoretical theories in study on thermodynamic properties of metals and alloys

Defects in general and vacancies in particular have a very important influence on the properties of metals and alloys at high temperatures. Equilibrium vacancy concentrations at melting point have

orders of magnitude about 10^{-3} in low-melting metals and 10^{-2} in high-melting-point metals. The strong nonlinear effects in heat capacity and thermal expansion at high temperatures can be explained by the formation of point defects. At high pressures above 100 GPa, another type of defect is dislocation, which contributes significantly to the melting temperature of the crystal.

There are many theoretical methods to study the vacancy and thermodynamic properties of metals and alloys such as the planar wave method of *ab initio* combined with pseudo-harmonic Debye model, *ab initio* calculation combined with generelized gradient approximation, *ab initio* combines density functional theory with generalized gradient approximation, approach of co-existence phases, calculation of phase diagram, lattice Green function method, modified embedded atomic method, machine learning method, etc. Each method has its own advantages and disadvantages when applied to multi-component systems at high temperature and pressure.

1.3. Statistical moment method

SMM is based on the following traceability formula for moments

$$\left\langle \hat{K}_{n+1} \right\rangle_a = \left\langle \hat{K}_n \right\rangle_a \left\langle \hat{Q}_{n+1} \right\rangle_a + \theta \frac{\partial \left\langle \hat{K}_n \right\rangle_a}{\partial a_{n+1}} - \theta \sum_{m=0}^{\infty} \frac{B_{2m}}{(2m)} \left(\frac{i\hbar}{\theta} \right)^{2m} \left\langle \frac{\partial \hat{K}_n^{(2m)}}{\partial a_{n+1}} \right\rangle_a . \quad (1.44)$$

This formula allows to determine the high-order moments over the lower-order moments, which can even be expressed in terms of the first-order moment.

CHAPTER 2
THERMODYNAMIC THEORY OF CUBIC DEFECTIVE BINARY ALLOY

In chapter 2, we use SMM and coordinate sphere method to derive general analytic expressions of free energy, displacement of particles from lattice node, mean nearest neighbor distance between two atoms, equilibrium vacancy concentration and thermodynamic quantities for defective interstitial alloy AC and perform numerical calculations to alloys AuSi and PtSi alloys. Part of the content of this chapter is published in [CT2, CT3, CT5]

2.1. Cubic perfect interstitial alloy AC

2.1.1. Alloy model

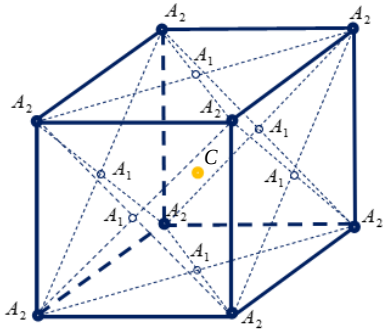

Fig. 2.1. *Model of FCC interstitial alloy AC*

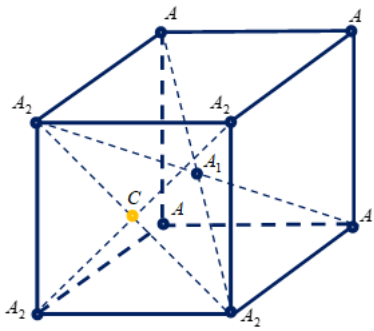

Fig. 2.2. *Model of BCC interstitial alloy AC*

For FCC lattice, $c_A = 1 - 15c_C$, $c_{A_1} = 6c_C$, $c_{A_2} = 8c_C$,

For BCC lattice, $c_A = 1 - 7c_C$, $c_{A_1} = 2c_C$, $c_{A_2} = 4c_C$

2.1.2. Helmholtz free energy

$$\Psi_{AC} = N\psi_{AC} = N \sum_{X=A,C,A_1,A_2} c_X \psi_X - TS_c^{AC},$$

$$\Psi_X = N\psi_X = U_{0X} + \Psi_{0X} + \frac{3N\theta^2}{k_X^2}\left[\gamma_{2X}Y_X^2 - \frac{2\gamma_{1X}}{3}\left(1+\frac{Y_X}{2}\right)\right] +$$
$$+\frac{6N\theta^3}{k_X^4}\left[\frac{4}{3}\gamma_{2X}^2 Y_X\left(1+\frac{Y_X}{2}\right) - 2\left(\gamma_{1X}^2 + 2\gamma_{1X}\gamma_{2X}\right)\left(1+\frac{Y_X}{2}\right)(1+Y_X)\right], \quad (2.1)$$

2.1.3. Cohesive energy and alloy parameters

The cohesive energy u_0 and crystal parameters $k, \gamma_1, \gamma_2, \gamma$ for main metal atom A in clean metal A, interstitial atom C, main metal atom A_1 at body center or face center, main metal atom A_2 in vertice of cubic unit cell in alloy AC are determined by SMM and in two or three coordinate sphere approximations (formulas (2.2) to (2.39).

2.1.4. Mean nearest neighbor distance between two atoms

The nearest neighbor distance $r_{1X}(P,0)$ $(\mathrm{X} = \mathrm{A}, \mathrm{A}_1, \mathrm{A}_2, \mathrm{C})$ is determined from the equation of state

$$Pv = -r_1\left(\frac{1}{6}\frac{\partial u_0}{\partial r_1} + \frac{\hbar\omega_0}{4k}\frac{\partial k}{\partial r_1}\right). \quad (2.41)$$

The nearest neighbor distances are determined by

$$r_{1C}(P,T) = r_{1C}(P,0) + y_{A_1}(P,T), r_{1A}(P,T) = r_{1A}(P,0) + y_A(P,T),$$
$$r_{1C}(P,T) = r_{1C}(P,0) + y_{A_1}(P,T), r_{1A}(P,T) = r_{1A}(P,0) + y_A(P,T), \quad (2.42)$$
$$\overline{r_{1A}(P,T)} = \overline{r_{1A}(P,0)} + \overline{y(P,T)}, \overline{r_{1A}(P,0)} = (1-c_C)\, r_{1A}(P,0) + c_C r'_{1A}(P,0),$$
$$\overline{y(P,T)} = c_A y_A(P,T) + c_C y_C(P,T) + c_{A_1} y_{A_1}(P,T) + c_{A_2} y_{A_2}(P,T), \quad (2.43)$$

2.2. Cubic defective interstitial alloy AC

2.2.1. Helmholtz free energy

$$\Psi_{AC}^R = N\left\{\sum_{X=A,C,A_1,A_2}\left\{\left[1 - n_v n_1 + n_v\left(B_X - 1\right)\right]c_X\psi_X + n_v n_1 c_X \psi_X^{(1)}\right\}\right\} -$$
$$-T\left(S_c^{AC*} + S_c^{AC}\right). \quad (2.50)$$

2.2.2. Displacement of atom from equilibrium position

$$y = \frac{1}{N}\left[\left(N - n_1 n - n_2 n\right) y_0 + n_1 n y_1\right] \tag{2.51}$$

2.2.3. Equilibrium vacancy concentration

$$n_v^{AC} = n_v^A \exp\left(-\frac{c_C g_v^f(C)}{k_{\mathrm{Bo}} T}\right),\ n_v^A = \exp\left(-\frac{\sum_{X=A,C,A_1,A_2} c_X g_v^f(X)}{k_{\mathrm{Bo}} T}\right) \tag{2.69}$$

2.3. Thermodynamic quantities

$$\chi_{TAC}^R = \frac{3\left(\frac{a_{AC}}{a_{0AC}}\right)^3}{2P + \frac{a_{AC}^2}{V_{AC}} \frac{1}{3N}\left(\frac{\partial^2 \Psi_{AC}^R}{\partial a_{AC}^2}\right)_T}, \tag{2.70}$$

$$\alpha_{TAC}^R = -\frac{\sqrt{2} k_{\mathrm{Bo}} \chi_{TAC}^R}{3 a_{AC}} \frac{1}{3N} \frac{\partial^2 \Psi_{AC}^R}{\partial \theta \partial a_{AC}}, \tag{2.71}$$

$$C_{VAC}^R = N \sum_{X=A,C,A_1,A_2} \left\{\left[1 - n_v n_1 + n_v\left(B_X - 1\right)\right] c_X C_{VX} + n_v n_1 c_X C_{VX}^{(1)}\right\}, \tag{2.74}$$

2.4. Numerical results for thermodynamic quantities of AuSi, PtSi

2.4.1. Interaction potential between atoms in interstitial alloy

$$\varphi(r) = \frac{D}{n-m}\left[m\left(\frac{r_0}{r}\right)^n - n\left(\frac{r_0}{r}\right)^m\right]. \tag{2.84}$$

2.4.2. Numerial results for AuSi *and* PtSi

For Au in AuSi at $P = 0$ in the temperature range from 800 to 1300 K, the equilibrium vacancies concentration increases from 10^{-5} to 10^{-3}. This is in agreement with experiments. n_v decreases markedly with Si concentration. When P (or T) increases, the fluctuations increase more strongly and make n_v also increase strongly. This result is consistent with experiments. Since in the low T and P regions, n_v is very small, then the crystal can be considered as ideal. But in the high T and P regions, the influence of n_v on the thermomechanical properties of the crystal is significant.

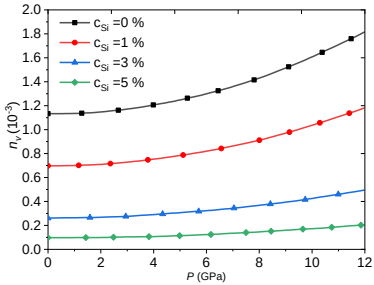

Figure 2.3. $n_v(P,c_{Si})$for AuSi (D) at T =1200 K

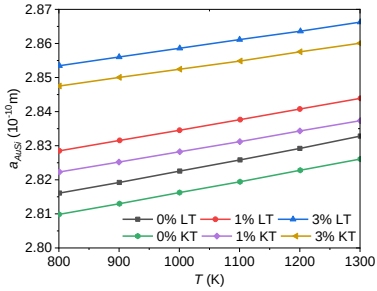

Figure 2.4. $a(T, c_{Si})$ for AuSi at P = 12 GPa

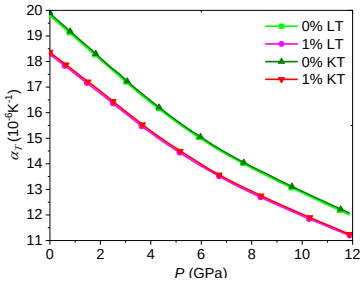

Figure 2.7. $\alpha_T(P, c_{Si})$ for AuSi at T = 1200 K

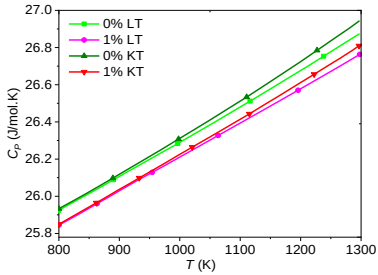

Figure 2.8. $C_P(T, c_{Si})$ for AuSi at P = 12 GPa

As T increases, the mean nearest neighbor distance a, the thermal expansion coefficient α_T and the isostatic heat capacity C_P increase, especially α_T. As P increases, these quantities both decrease. The higher the T and P, the smaller the c_{Si}, the stronger the influence of the vacancy on the thermomechanical properties of the crystal.

For Au, the maximum error between calculation and experiment is 4.4% for α_T at 700 K and 5.4% for C_P at 1200 K, which means that there is a good agreement between calculation and experiment. over a wide temperature range. The calculation results for C_P of Au with vacancy are better than the calculation results for C_P of the perfect Au. However, the calculation results for the α_T of Au with vacancies are worse than the results for the α_T of the perfect Au although still within the allowable error range.

CHAPTER 3
THERMODYNAMIC THEORY OF CUBIC DEFECTIVE SUBSTITUTIONAL AND INTERSTITIAL TERNARY ALLOY

In chapter 3, we also use SMM and coordinate sphere method to derive general analytic expressions of free energy, displacement of particles from lattice node, mean nearest neighbor between two atom, equilibrium vacancy concentration and thermodynamic quantities for cubic defective substitutional and interstitial alloy ABC and perform numerical calculations for alloys AuCuSi, PtCuSi alloys, FeCrSi and VWSi. Part of the content of this chapter is published in [CT1, CT4, CT6].

3.1. Cubic perfect substituitonal and interstitial alloy ABC

3.1.1. Alloy model

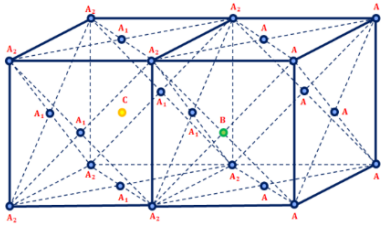

Fig. 3.1. *Model of FCC substitutional and interstitial alloy ABC*

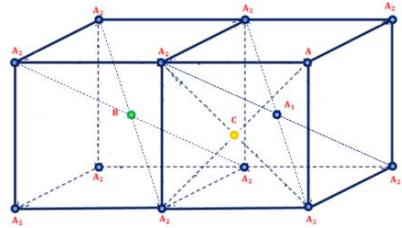

Fig. 3.2. *Model of BCC substitutional and interstitial alloy ABC*

3.1.2. Helmholtz free energy

$$\Psi_{ABC} = \Psi_{AC} + Nc_B\left(\psi_B - \psi_A\right) + TS_c^{AC} - TS_c^{ABC} = \\ = N \sum_{X=A,B,C,A_1,A_2} c_X\psi_X + TS_c^{AC} - TS_c^{ABC}, \qquad (3.1)$$

For FCC lattice, $c_A = 1 - 15c_C$, $c_{A_1} = 6c_C$, $c_{A_2} = 8c_C$

For BCC lattice, $c_A = 1 - 7c_C, c_{A_1} = 2c_C, c_{A_2} = 4c_C$

3.1.3. Cohesive energy and alloy parameters

The expressions of the cohesive energy and the crystal parameters for atoms C, A_1, A_2 of the interstitial alloy AC in the substitutional and interstitial alloy ABC are the same as in chapter 2.

3.1.4. Mean nearest neighbor distance between two atoms

$$a_{ABC} = c_{AC} a_{AC} \frac{B^R_{TAC}}{B^R_T} + c_B r_{1B} \frac{B^R_{TB}}{B^R_T} \tag{3.2}$$

3.2. Cubic defective substitutional and interstitial alloy ABC

3.2.1. Helmholtz free energy

$$\Psi^R_{ABC} = N\Psi^R_{ABC} = N \sum_{X=A,B,C,A_1,A_2} \left\{ \left[1 - n_v n_1 + n_v \left(B_X - 1 \right) \right] c_X \psi_X + n_v n_1 c_X \psi^{(1)}_X \right\} -$$

$$-T\left(S_c^{ABC*} + S_c^{ABC} - S_c^{AC} \right) \tag{3.9}$$

3.2.2. Displacement of atom from equilibrium position

$$y = \frac{1}{N} \left[\left(N - n_1 n - n_2 n \right) y_0 + n_1 n y_1 \right], \tag{3.10}$$

3.2.3. Equilibrium vacancy concentration

$$n_v^{ABC} = n_v^A \exp\left(-\frac{c_B g_v^f(B)}{k_{Bo} T} \right) \exp\left(-\frac{c_C g_v^f(C)}{k_{\mathrm{Bo}} T} \right), \tag{3.13}$$

3.3. Thermodynamic quantities

$$\chi^R_{TABC} = \frac{3\left(\frac{a_{ABC}}{a_{0ABC}} \right)^3}{2P + \frac{a^2_{ABC}}{V_{ABC}} \frac{1}{3N} \left(\frac{\partial^2 \Psi^R_{ABC}}{\partial a^2_{ABC}} \right)_T}, \tag{3.14}$$

$$\alpha^R_{TABC} = -\frac{\sqrt{2} k_{\mathrm{Bo}} \chi^R_{TABC}}{3 a_{ABC}} \frac{1}{3N} \frac{\partial^2 \Psi^R_{ABC}}{\partial \theta \partial a_{AC}}, \tag{3.15}$$

$$C^R_{VAC} = N \sum_{X=A,B,C,A_1,A_2} \left\{ \left[1 - n_v n_1 + n_v \left(B_X - 1 \right) \right] c_X C_{VX} + n_v n_1 c_X C^{(1)}_{VX} \right\}, \tag{3.18}$$

$$C^R_{PABC} = C^R_{VABC} + \frac{9TV_{ABC}\alpha^{R2}_{TABC}}{\chi^R_{TABC}}. \quad (3.19)$$

3.4. Numerical results for AuCuSi, PtCuSi, FeCrSi and VWSi

3.4.1. Thermodynamic numerical results of AuCuSi, PtCuSi *with FCC structure*

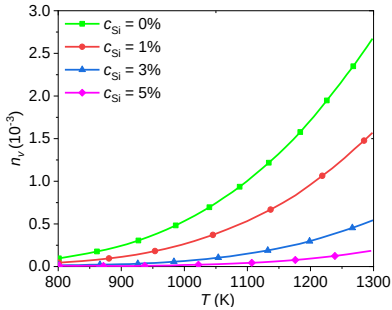

Figure 3.3. $n_v(T, c_{Si})$ for AuCuSi at P = 8 GPa, c_{Cu} = 10%

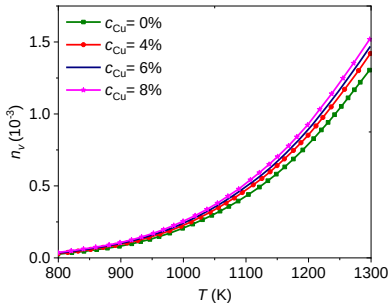

Figure 3.4. $n_v(T, c_{Cu})$ for AuCuSi at P = 8 GPa, c_{Si} = 1%

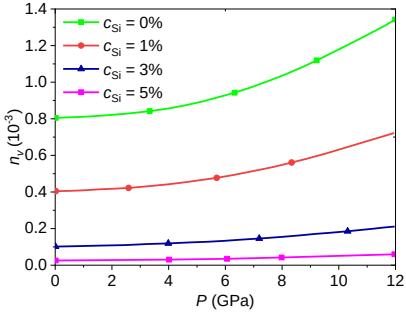

Figure 3.5. $n_v(P, c_{Si})$ for AuCuSi at T = 1100 K, c_{Cu} = 10%

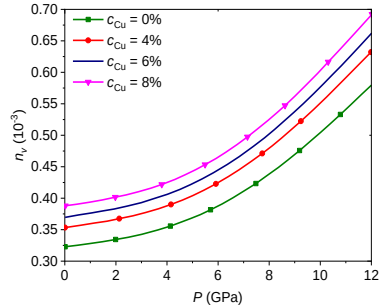

Figure 3.6. $n_v(P, c_{Cu})$ *đối với* for AuCuSi at T = 1000 K, c_{Si} = 1%

For AuCuSi in the range of pressure from zero to 12 GPa and in the range of temperature from 800 to 1300K, the equilibrium vacancy concentration range falls between 10^{-5} and 10^{-3}. This result is in good agreement with the experiment for Au at high temperatures and pressures. Besides, n_v strongly depends on T and P. As T and P increase, n_v also increases. Near the melting point of Au, n_v increases sharply. Since at low T and P, n_v is very small, then the alloy is

considered ideal and at high T and P, n_v is significant and the influence of the vacancy cannot be ignored. n_v also changes markedly with c_{Si}. As c_{Si} increases, n_v decreases sharply. Consider the effect of c_{Cu} on n_v. Although c_{Cu} is much larger than c_{Si}, c_{Cu} does not significantly change the n_v and other properties of the alloy.

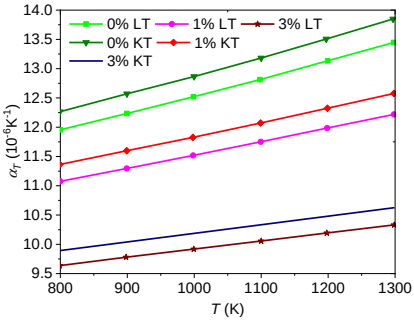

Figure 3.10. $\alpha_T(T, c_{Si})$ for AuCuSi at P = 12 GPa, c_{Cu} = 10%

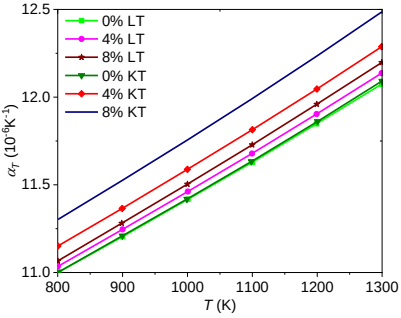

Figure 3.11. $\alpha_T(T, c_{Cu})$ for AuCuSi at P = 12 GPa, c_{Si} = 1%

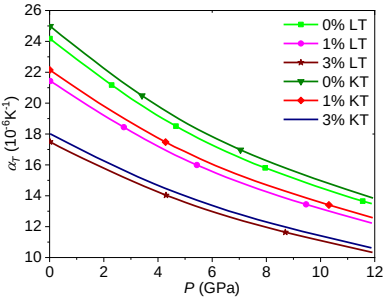

Figure 3.12. $\alpha_T(P, c_{Si})$ for AuCuSi at T = 1300 K, c_{Cu} = 10%

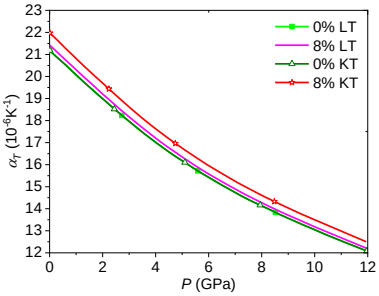

Figure 3.13. $\alpha_T(P, c_{Cu})$ for AuCuSi at T = 1300 K, c_{Si} = 1%

Consider the mean nearest neighbor distance a in AuCuSi and PtCuSi. At the same T, P and doping concentrations, a of the defective alloys are less than a of the perfect alloys.

Consider the dependence of α_T on T and P. At the same P and doping concentration, α_T increases with T, but at the same T and doping concentration, α_T decreases with P. This is in agreement with

experiments. At the same T and P as c_{Si} increases, α_T decreases. Considering the perfect alloy or the defective alloy, although the dependence of α_T on c_{Cu} is less than that of α_T on c_{Si} but c_{Cu} plays an important role in making the difference between α_T of the perfect alloy and α_T of the defective alloy as well as other properties. If the interstitial atom interferes with the vacancy formation, the substitutional atom favors the vacancy formation.

The dependence of C_P on T, P and doping concentration for AuCuSi and PtCuSi is the same as α_T. However, at the same doping concentration, the variation of C_P with respect to T and P is not as strong as α_T. This is consistent with the theory of quantum statistical physics and experiments when studying solids in the high T and P regions.

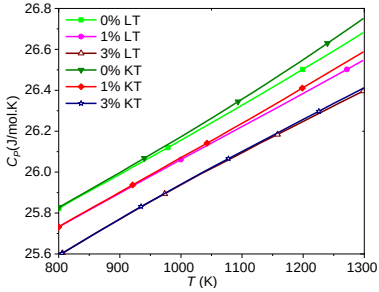

Figure 3.18. $C_P(T, c_{Si})$ for AuCuSi at P = 12 GPa, c_{Cu} = 10%

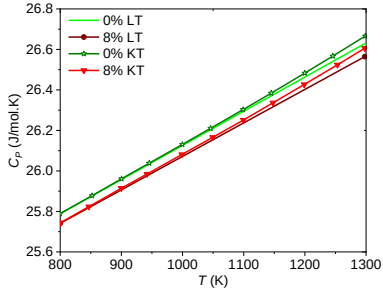

Figure 3.19. $C_P(T, c_{Cu})$ for AuCuSi at P = 12 GPa, c_{Si} = 1%

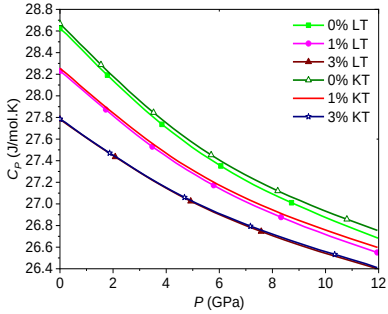

Figure 3.20. $C_P(P, c_{Si})$ for AuCuSi at T = 1300 K, c_{Cu} = 10%

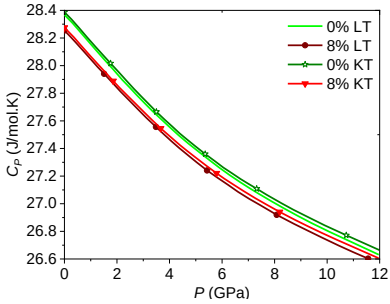

Figure 3.21. $C_P(P, c_{Cu})$ for AuCuSi at T = 1300 K, c_{Si} = 1%

3.4.2. Thermodynamic numerical results of **FeCrSi, VWSi** *with BCC structural*

For FeCrSi, n_v is strongly dependent on P and T. At the same c_{Cr} and c_{Si} as P (or T) increases, n_v also increases significantly. In the low P and T regions, n_v is very small and the alloy is considered ideal, while in the high P and T regions, n_v increases exponentially and changes the properties of the alloy. n_v increases with P not as fast as with T but the change of n_v is obvious. This result is consistent with experiments because as T and P increase, the lattice fluctuations increase and create favorable conditions for the vacancy formation.

When adding Si or Cr to the Fe lattice, n_v decreases sharply. Cr is often added to Fe to produce steel with high strength and hardness, that is, the cohesive energy u_0 between the atom and the lattice becomes stronger. This impedes the formation of a defect node. However, c_{Cr} does not reduce n_v as strongly as c_{Si}.

The mean nearest neighbor distance a of FeCrSi and VWSi all increase with T, decrease with P, increase with c_{Si} and decrease with c_{Cr} or c_W. a for defective alloys is less than a for perfect alloys respectively.

Consider the thermal expansion coeficient α_T and the heat capacity at constant pressure C_P of FeCrSi and VWSi. At the same P, c_{Si} and c_{Cr} (or c_W) as T increases, α_T increases. At the same P, c_{Si} and c_{Cr} (or c_W) as T increases, C_P also increases with T but this increase is not as strong as the increase of α_T with T. At the same T when P or c_{Si} (or c_{Cr}) increases, α_T and C_P both decrease. C_P of defective alloys is smaller than that of perfect alloys. α_T of defective alloys is larger than that of perfect alloys.

CHAPTER 4
MELTING AND STRUCTURAL PHASE TRANSITION OF CUBIC DEFECTIVE TERNARY AND BINARY INTERSTITIAL ALLOYS

In chapter 4, we build the theory of melting and structural phase transition of cubic defective interstitial alloys AC and ABC using SMM and perform numerical calculations for the melting temperatures of alloys FeC, TaSi, WSi and structural phase transition temperature of metal Fe. The contents of chapter 4 are published in [CT3, CT4, CT5].

4.1. Theory of melting and structural phase transition for cubic defective interstitial alloy AC

4.1.1. Melting theory of cubic defective interstitial alloy AC

$$\left(\frac{\partial P}{\partial v}\right)_{T=T_s} = 0, \tag{4.1}$$

$$T_s = \frac{a_s}{18k_B\gamma_G\left(P,T_s\right)}\left(\frac{\partial u_0}{\partial a}\right)_{T=T_s} + \left(\frac{\partial T}{\partial P}\right)_v P, \tag{4.3}$$

$$T_m \approx T_s + \frac{a_m - a_s}{k_B\gamma_G\left(P,T_s\right)}\left\{\frac{Pv\left(P,T_s\right)}{a_s} + \frac{1}{18}\left[\left(\frac{\partial u_0}{\partial a}\right)_{T=T_s} + a_s\left(\frac{\partial^2 u_0}{\partial a^2}\right)_{T=T_s}\right]\right\}, \tag{4.4}$$

$$T_m(P) = T_m(0)\left[\frac{a(P,300\mathrm{K})}{a(P=0,300\mathrm{K})}\right]^2 \frac{k(P,300\mathrm{K})}{k(P=0,300\mathrm{K})}, \tag{4.6}$$

$$T_m(P) = T_m(0)\frac{G(P,300\mathrm{K})}{G(P=0,300\mathrm{K})}\left[\frac{B_T(P,300\mathrm{K})}{B_T(P=0,300\mathrm{K})}\right]^{-\frac{1}{b}}, \tag{4.7}$$

$$T_m^R = T_m - \left(\frac{\partial T}{\partial n_v}\right)_{P,V} n_v(T_m) = T_m - \frac{T_m^2}{\frac{T_m}{4}\frac{\partial u_0}{\partial \theta} - \frac{u_0}{4k_B}}, \tag{4.10}$$

$$T_S(0) = \frac{a_{AB}}{18\gamma_G^T k_{\mathrm{Bo}}}\sum_X \left\{\left[1 - n_v n_1 + n_v\left(B_X - 1\right)\right]c_X \frac{\partial U_{0X}}{\partial a_X} + n_v n_1 c_X \frac{\partial U_{0X}^{(1)}}{\partial a_X}\right\}, \tag{4.20}$$

$$T_m(P) = \frac{T_m(0)B_0^{\frac{1}{B_0'}}}{G(0)} \cdot \frac{G(P)}{(B_0 + B_0'P)^{\frac{1}{B_0'}}}. \quad (4.31)$$

4.1.2. Structural phase transition theory

$$T_{AC}^{R\alpha-\beta}(P=0) = \left|\frac{\Delta E_{AC}^R}{\Delta S_{AC}^R}\right| = \left|\frac{E_{AC}^{R\alpha} - E_{AC}^{R\beta}}{S_{AC}^{R\alpha} - S_{AC}^{R\beta}}\right|, \quad (4.33)$$

$$T_{AC}^{R\alpha-\beta}(P) = \left|\frac{\Delta E_{AC}^R + P\Delta V_{AC}}{\Delta S_{AC}^R}\right| = \left|\frac{E_{AC}^{R\alpha} - E_{AC}^{R\beta} + P\left(V_{AC}^{\alpha} - V_{AC}^{\beta}\right)}{S_{AC}^{R\alpha} - S_{AC}^{R\beta}}\right| \quad (4.39)$$

4.2. Theory of melting and structural phase transition for cubic defective substitutional and interstitial alloy ABC

4.2.1. Melting theory of cubic defective interstitial alloy ABC

We also apply the melting theory mentioned in section 4.1.1. for cubic defective interstitial alloy ABC.

4.2.2. Structural phase transition theory

$$T_{ABC}^{R\alpha-\beta}(P=0) = \left|\frac{\Delta E_{ABC}^R}{\Delta S_{ABC}^R}\right| = \left|\frac{E_{ABC}^{R\alpha} - E_{ABC}^{R\beta}}{S_{ABC}^{R\alpha} - S_{ABC}^{R\beta}}\right|, \quad (4.54)$$

$$T_{ABC}^{R\alpha-\beta}(P) = \left|\frac{\Delta E_{ABC}^R + P\Delta V_{ABC}}{\Delta S_{ABC}^R}\right| = \left|\frac{E_{ABC}^{R\alpha} - E_{ABC}^{R\beta} + P\left(V_{ABC}^{\alpha} - V_{ABC}^{\beta}\right)}{S_{ABC}^{R\alpha} - S_{ABC}^{R\beta}}\right|. \quad (4.60)$$

4.3. Numerical results of melting temperature and structural phase transition temperature

4.3.1. Numerical results for melting temperatures of alloys TaSi, WSi *and FeC*

According to Fig.4.3, when c_{Si} increases from 0 to 7%, T_m of TaSi decreases from 3210 to 2423K according to SMM calculation for perfect alloy model, from 3031 to 2310K according to SMM calculation for defective alloy model and from 3247 to 2533K according to CALPHAD [*Journal of Phase Equilibria and Diffusion*, 30(5)(2000)564].

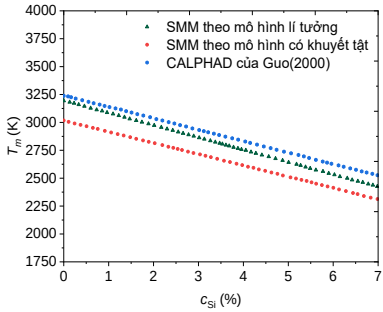

Figure 4.3. $T_m(c_{Si})$ for TaSi at $P = 0$

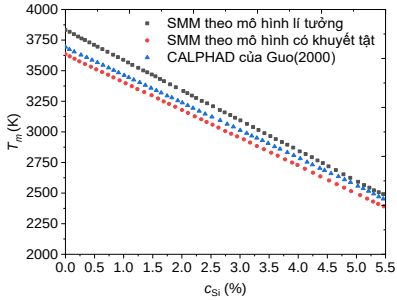

Figure 4.4. $T_m(c_{Si})$ for WSi at $P = 0$

According to Fig.4.4, when c_{Si} increases from 0 to 5.5%, T_m of WSi decreases from 3810 to 2459K according to the calculation of SMM for the perfect alloy model, from 3609 to 2366K according to the calculation of SMM for the defective alloy model and from 3695 to 2460K according to CALPHAD[*Journal of Phase Equilibria and Diffusion*, 30(5)(2000)564]. The interstitial atom makes the crystal compaction coefficient larger and the n_v at the melting point decreases with the increase of c_{Si}. These reasons lead to a smaller value for the slope of the melting curve. The SMM calculations for the melting curve slope of the defect crystal are in good agreement with the corresponding results from CALPHAD.

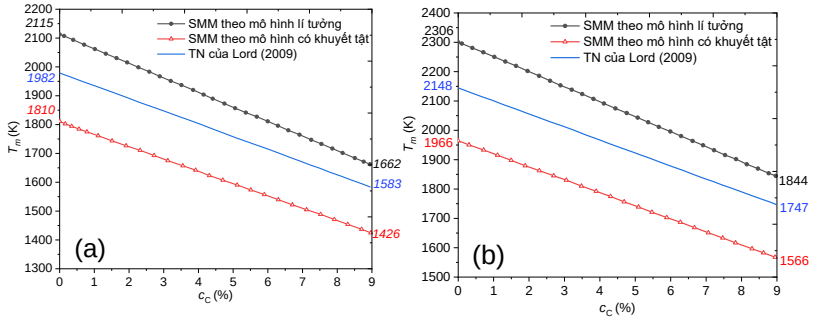

Figure 4.8. Influence of interstitial atom C on melting temperature of γ-FeC at $P = 0$ (Figure 4.8a) and $P = 5$ GPa (Figure 4.8b) calculated by SMM and from experiments

According to Fig.4.8, the interstitial atom C causes the melting temperature of γ-Fe to decrease markedly. In Fig.4.8a for γ-FeC at P = 0, $\Delta T_m / \Delta c_C = -50.33\text{K}/\%$ calculated SMM for perfect γ-FeC, $\Delta T_m / \Delta c_C = -44.33\text{K}/\%$ calculated SMM for defective γ-FeC and $\Delta T_m / \Delta c_C = -42.67\text{K}/\%$ from experiments of Lord *et al.* [*Earth and Planetary Science Letters*, 284(1-2)(2009)157]. According to Fig.4.8b for P = 5 GPa, $\Delta T_m / \Delta c_C = -51.22\text{K}/\%$ calculated by SMM for perfect γ-FeC, $\Delta T_m / \Delta c_C = -44.56\text{K}/\%$ calculated by SMM for defective γ-FeC and $\Delta T_m / \Delta c_C = -44.44\text{K}/\%$ from experiments of Lord *et al.* [*Earth and Planetary Science Letters*, 284(1-2)(2009)157].

4.3.2. Numerical results for α-γ structural phase transition temperatures of Fe

According to Fig. 4.13, the results calculated by SMM are in good agreement with experiments [*Journal of Applied Physics*, 36 (2) (1965) 616; *Metallurgical Transactions*, 4 (11) (1973) 2657]. All errors are less than 10% over a wide range of pressures from 0 to 11 GPa

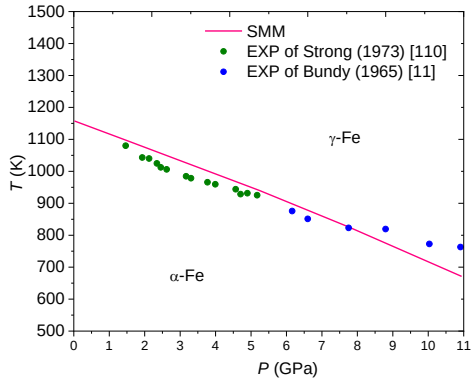

Fig.4.13. The structural phase transition curve between α-Fe and γ-Fe

GENERAL CONCLUSIONS

The thesis uses the SMM to build the theory of thermodunamics, melting and structural phase transition of cubic defective interstitial alloy AC and substitutional and interstitial alloy ABC at zero pressure and under pressure and apply the obtained theory to calculate numerically for some metals and alloys. The thesis has achieved the following main results:

1. On the basis of the model of cubic perfect interstitial alloy AC and substitutional and interstitial alloy ABC, the general analytic expressions of the displacement of the atom from the lattice node, the mean nearest neighbor distance between two atoms, the equilibrium vacancy concentration, the Helmholtz free energy, thermodynamic quantities, the absolute stability temperature of alloy state, the melting temperature and the structural phase transition temperature depending on temperature, pressure, concentration of substitutional atoms, concentration of interstitial atoms and equilibrium vacancy concentration are derived for cubic defective interstitial alloy AC and substitutional and interstitial alloy ABC. The theories of thermodynamics, melting and structural phase transitions of cubic defective metal, binary interstitial alloy, binary substitutional alloy are limit cases of the theory of thermodynamics, melting and structural phase transitions of cubic defective ternary substitutional and interstitial alloy corresponding for zero concentrations of substitutional atoms and interstitial atoms, zero concentration of substitutional atoms and zero concentrations of interstitial atoms.

2. Apply the obtained theoretical results to calculate numerically for some thermodynamic quantities of AuSi, PtSi, FeCrSi, VWSi,

AuCuSi, PtCuSi, the melting temperature of TaSi, WSi, γ-FeC and the BCC-FCC structural phase transition temperature of Fe with the pair potential Mie-Lennard-Jones *n-m* depending on temperature, pressure, concentration of substitutional atoms, concentration of interstitial atoms and equilibrium vacancy concentration. The results obtained by the SMM are in good agreement with other calculations using the *ab initio*, the Lindemann law, the MD, etc. and the experimental data. Other calculated results predict future experimental results.

Many numerical results obtained by the SMM have good agreement with experimetns and in many cases have better agreement than those calculated by other methods. The error compared with the experiment is only about 10%. That proves that the method that we have used for research in the thesis has high reliability.

The success of the thesis contributes to perfecting and developing the application of SMM to study the properties of interstitial alloy materials taking into account the influence of the anharmonicity effect of lattice vibrations.

LIST OF PUBLISHED PAPERS OF THE THESIS

1. Nguyen Quang Hoc, Vu Dinh Lam, Pham Thi Minh Hanh, Tran Dinh Cuong and **Le Hong Viet** (2018). Heat capacity at constant pressure of defective FCC substitutional alloy AB with interstitial atom C, *Proc.the 9th International Workshop on Advanced Materials Science and Nanotechnology (IWAMSN 2018)*, Ninh Binh province, Vietnam, 7-11th November 2018, pp.49-56.

2. Nguyen Thi Hoa, Nguyen Quang Hoc, Gelu Coman, Tran Dinh Cuong and **Le Hong Viet** (2018). Thermodynamic property of FCC interstitial alloy AuSi with defects, *Proceedings of the 8th International Conference on Material Science and Engineering (UGALMAT 2018)*, 11 – 13 October, 2018, "Dunarea de Jos" University of Galati, Romania, *IOP Conference Series: Materials Science and Engineering* **485**, 012018.

3. Nguyen Quang Hoc, Bui Duc Tinh, Tran Dinh Cuong and **Le Hong Viet** (2019). Study on the melting of defective interstitial alloys TaSi and WSi with BCC structure. *Journal of the Korean Physical Society* **71**(8),pp.801-805.

4. Nguyen Quang Hoc, Dinh Quang Vinh, **Le Hong Viet**, Ta Dinh Van and Pham Thanh Phong (2019), Study on Structural Phase Transitions in Defective and Perfect Substitutional Alloys AB with Interstitial Atoms C under Pressure, *HNUE JOURNAL OF SCIENCE, Natural Sciences*, **64**(6),pp.57-67.

5. Nguyen Quang Hoc, **Le Hong Viet** and Nguyen Trong Dung (2019), On the melting of defective FCC interstitial alloy γ-FeC under pressure up to 100 GPa, *Journal of Electronic Materials*, **49**(2),pp.910-916.

6. **Le Hong Viet** and Nguyen Quang Hoc (2021), Equilibrium vacancy concentration and thermodynamic quantities of FCC defective alloys AuCuSi and PtCuSi under pressure, *HNUE JOURNAL OF SCIENCE, Natural Sciences*, **66**(3),pp.38-51;